Chapter 2
Rectangular DRA Resonant Modes and Sources

Abstract Basics of resonant modes have been described. Their mathematical analysis for generation of different resonant modes have been presented in this chapter. Realization of resonant modes based on MATLAB has also been worked. Modes are generated by applying voltage source. Various types of resonant modes have been described along with all possible applications.

Keywords Cavity resonator · Resonant modes · Type of modes · Wave guide analysis · Mathematical description of resonant modes · Simulated work

2.1 Introduction

In the early 1960s, Okaya and Barash [1] reported the first ever DRA in the form of a single-crystal TiO_2. Since then, no rigorous theoretical analysis has been developed so far in the literature to evaluate the resonant modes in Rectangular DRA. Based on Cherenkov principle of radiations, an external electric field brings the charges of the molecules of the dielectric into a certain ordered arrangement in space and creates acceleration phenomenon in dielectric material itself. The dielectric polarization P is equal to the total dipole moment induced in the volume of the material by the electric fields. In most cases, the magnitude of polarization is directly proportional to the intensity of the electric field at a given point of a dielectric. The relative permittivity is related to the dielectric susceptibility. A dielectric resonator is defined as "object of dielectric material which *functions as a resonant cavity by means of reflections at the dielectric air interface*." The discontinuity of the relative permittivity at the resonator surface allows a standing electromagnetic wave to be supported in its interior at a particular resonant frequency, thereby leading to maximum confinement of energy within the resonator.

Certain fields distribution or modes will satisfy Maxwell's equations and boundary conditions. Resonant modes are field structures that can exist inside the DRA. Modes are the pattern of motion which repeat itself sinusoidally. Infinite number of modes can excited at same time. Any motion is superposition or

R.S. Yaduvanshi and H. Parthasarathy, *Rectangular Dielectric Resonator Antennas*, DOI 10.1007/978-81-322-2500-3_2

weighted sum of all the modes at any instant of time by combining amplitudes and phases. As in the case of all resonant cavities, there are many possible resonant modes that can be excited in dielectric resonators. The boundary conditions are $n \cdot H = 0$; where H denotes the electric field intensity and n denotes the normal to the surface of the resonator.

And, $n \times E = 0$, is not necessarily satisfied at all the surfaces of the RDRA by all the modes. Different resonant modes have distinct electromagnetic field distributions within the DRA, and each mode may provide a different radiation pattern.

Operation of DRA is based on the process that if excitation is applied, then a high magnetic field is created inside the dielectric object placed on a ground plane. Phenomena which occur like a charge particle passing to the field create the physical environment like any metal ball passing through liquid. Thus, there will be change in the field, contraction, and expansion, which causes fringing effect. This way dielectric object starts to radiate. Another phenomenon that occurs is that there might be reflection of the field from sidewalls of dielectric object due to change in the refractive index of the medium. The dielectric object acts as an oscillator.

Theory of characteristic modes can be applied in the design of antenna or DRA. These modes give insight into physical phenomenon taking place inside device in terms of current vectors as maxima and minima. This helps to locate the feeding point and desired dimension of RDRA.

In 1968, modes were introduced by Garbacz and later by Harrington. Inagaki gave simpler theory on modes for radiation mechanism in an antenna. It requires lot of computation, for loading quality factor, double feeding to improve bandwidth, and circular polarization. Characteristic modes are current modes or eigenvectors, which are the solution of characteristic equation. These are orthogonal functions that can predict total current on surfaces of body of the antenna. Also, desired mode can be excited for specific radiating pattern. Excitation of mode mainly depends on feeding arrangement, geometry of the device, and dielectric material used. In time domain, varying electric field can produce magnetic fields and vice versa. By applying RF, excitation currents in RDRA get converted into surface current density distributed over the surfaces, i.e., RF excitation with proper impedance match can generates J. This probe current produced magnetic vector potential "A." The radiated magnetic fields are presented in the form E-electric field intensity using Lorentz gauge transformation. An antenna can propagate electromagnetic fields, if wave vector $k > k_c$. The cutoff wave vector k_c determines the cutoff frequency. There can be dominant resonant frequency or higher-order resonant frequency. The propagation takes place along x-axis if propagation constant $k > \frac{n\pi}{b}$. There will not be any propagation if $k \leq \frac{n\pi}{b}$, as it will lead to formation of standing waves. Similar conditions persist for propagation along y-axis and z-axis. Maxwell's equations define the behavior of electromagnetic wave propagation, while the solution of Maxwell equation is defined by Helmholtz equation. The radiated power is given by Parseval's power theorem. Half-wave Fourier analysis is used to determine the time domain behavior of antenna radiations. The magnitude and phase of the radiated field is given by Poynting vector ($S = E \times H$). The image theorem can be applied for antenna size reduction. It can be implemented by extending ground plane to an isolated RDRA. Resonance in RDRA is created due to formation of standing waves inside the device. Frequency ω_{mnp} is the spectral solution of an antenna, and this can determine the base half-wave Fourier analysis. Principle of orthonormality is used to determine radiation parameters by equating electric time average energy equal to magnetic time average energy by KAM (Kalmogorov–Arnold–Moser).

At any instant of time, n number of modes exist. The particular mode can be excited by increasing weighted amplitude of desired mode. More than one mode can also be excited into RDRA. Blocking modes can take place if E_z and H_z fields of same frequency are available in RDRA at any instant of time. Hence, mode spectrum will result into corresponding resonant frequency generation. Wave propagation can be defined by Helmholtz equation. The Maxwell's equation describes the behavior of electromagnetic fields and forms the basis of all EM classical phenomena. The size of antenna can be reduced to half by image theorem, converting isolated cavity into infinite ground plane. Dielectric resonator antenna is formed with high permittivity substrate. The abrupt change in permittivity due to change in medium forms standing waves. These waves establish resonance as they bounce back and forth in-between two walls due to fields perturbation. Modes are spectral resolution of electromagnetic fields of waves radiated by the RDRA. Modal excitation mainly depends on:

(a) Position of probe;
(b) Magnitude of probe current; and
(c) Phase of input current.

To compute resonant modes, vector principle of orthonormality on half-wave Fourier analysis has been applied, i.e., radiated magnetic energies time averaged are compared with applied electrical energies time averaged in the case of resonator antennas. More number of modes along z-axis in RDRA can be generated either by increasing electrical height "d" of RDRA or by increasing resonant frequency of DRA. Figure 2.1 depicts the prototype RDRA with moat under fabrication.

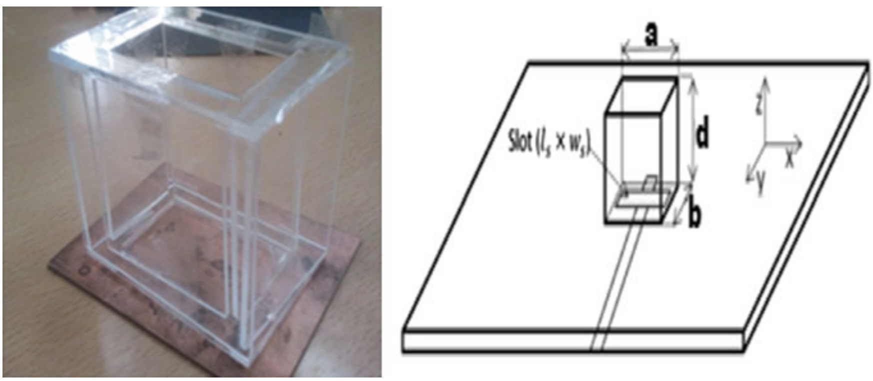

Fig. 2.1 RDRA prototype with neat sketch

Depending on the nature of the surfaces, different linear combinations of the $\pm\gamma$ modes are formed. The propagation constant (γ) itself is taking discrete values. This forces the natural frequencies of the field oscillations to take discrete values (*mnp*) indexed by three positive integers, namely m, n, and p. The solutions of the waveguide problem yield discrete values of γ, i.e., $\gamma(m, n, \omega)$ for a given frequency ω by applying boundary conditions to the electromagnetic fields on the sidewalls. The corresponding field amplitudes are solutions to the 2-D Helmholtz equations corresponding to the transverse Laplacian $\nabla_{\perp}^{2}$. These amplitudes are called “the waveguide modes” and are of the form given below in Sect. 2.2.

2.2 Type of Modes (TE, TM, HEM)

EM waves are of four types given below:
Transverse electric and magnetic (TEM) mode

- Transverse electric (TE) mode
- Transverse magnetic (TM) mode
- Hybrid electric and magnetic (HEM) or HE odd and EH even mode

Modes propagation depends mainly on following configuration:

1. Excitation
2. Dimensions
3. Coupling
4. Medium
5. Point of excitation
6. Input impedance

Cross-polarization solution can be the outcome of modes. They can be merged, separated and mixed depending upon the requirements. Half Fourier analysis can be used to describe modes of propagation and excitation. Even and odd modes can be studied. They can be analyzed with magnetic dipole moments. They help to predict far field radiation patterns. Modulated bandwidth and gain control can be achieved. High gain at higher modes can be used for hardware implementations. Device dimensions can be minimized by proper selection of modes for resonant frequencies. In case of milli metric (mm) wave, device size can be enlarged for easy hardware development or hardware implementation. The solution is based on waveguide method when boundaries have been all six electrical walls. The solution is based on solution of Maxwell’s equations and then restricted to given boundary conditions for confined modes of EM waves.

2.3 Solutions of Helmholtz Equation

Helmholtz equation solution with source

$$\nabla \times H = J + \frac{\partial D}{\partial t} \tag{2.1}$$

$$D = \epsilon E$$

$$B = \mu H = \nabla \times A$$

$$H = \frac{1}{\mu}(\nabla \times A)$$

Considering the sources to be natural time harmonic

$$E = E_m e^{j\omega t} \tag{2.2a}$$

$$H = H_m e^{j\omega t} \tag{2.2b}$$

Now,

$$\nabla \times E = -\frac{\partial B}{\partial t} \tag{2.3}$$

or

$$\nabla \times E = -j\omega\mu H = -j\omega(\nabla \times A)$$

$$\nabla \times (E + j\omega A) = 0 \tag{2.4}$$

Using vector identity

$$\nabla \times (-\nabla ø_e) = 0$$

$$E + j\omega A = -\nabla ø_e$$

$$E = -j\omega A - \nabla ø_e$$

Using the vector identity

$$\nabla \times (\nabla \times A) = \nabla(\nabla \times A) - \nabla^2 A \tag{2.5}$$

Now,

$$\nabla \times (\mu H) = \nabla(\nabla \times A) - \nabla^2 A$$

or

$$\mu(\nabla \times H) = \nabla(\nabla \times A) - \nabla^2 A$$

From Maxwell's fourth equation,

$$\nabla \times H = J + j\omega\epsilon E$$

or

$$\nabla \times \frac{B}{\mu} = J + j\omega\epsilon E$$

or

$$\nabla \times B = \mu J + j\omega\epsilon\mu E$$

or

$$\nabla \times (\nabla \times A) = \mu J + j\omega\epsilon\mu E$$

or

$$\nabla(\nabla \times A) - \nabla^2 A = \mu J + j\omega\epsilon\mu E$$

$$\nabla(\nabla \times A) - \nabla^2 A = \mu J + j\omega\epsilon\mu(-j\omega A - \nabla\varnothing_e)$$

or

$$\nabla(\nabla \times A) - \nabla^2 A = \mu J + \omega^2\epsilon\mu A - j\omega\mu\epsilon(\nabla\varnothing_e)$$

or

$$\nabla^2 A + k^2 A = -\mu J + j\omega\mu\epsilon(\nabla\varnothing_e) + \nabla(\nabla \times A)$$

or

$$\nabla^2 A + k^2 A = -\mu J + \nabla(j\omega\mu\epsilon\varnothing_e + (\nabla \times A))$$

where $k^2 = \omega^2\mu\epsilon$.

Using Lorentz condition, i.e.,

$$\nabla \times A = -j\omega\varepsilon\mu ø_e$$

or

$$ø_e = -\frac{1}{j\omega\mu\varepsilon}(\nabla \times A)$$

$$\nabla^2 A + k^2 A = -\mu J + \nabla(j\omega\mu\epsilon ø_e - j\omega\varepsilon\mu ø_e) \tag{2.6}$$

Hence, $\nabla^2 A + k^2 A = -\mu J$.

2.4 Rectangular Waveguide Analysis

Propagation in waveguide has been taken along z-axis, and all the four sidewalls of waveguide are PEC; the fields computed are as follows:

$$\begin{matrix} H_x & E_x \\ H_y & E_y \\ H_z & E_z \end{matrix}$$

$$E_z(x, y, z) = \sum_{m,n=1}^{\infty} C(m, n) \sin\left(\frac{m\pi x}{a}\right) \sin\left(\frac{n\pi y}{b}\right) \exp(-\gamma_{mn} z); \tag{2.7a}$$

$$E_{z,y} = \frac{\partial E_z}{\mathrm{d}y};$$

$$E_{z,x} = \frac{\partial E_z}{\mathrm{d}x}$$

$$H_z(x, y, z) = \sum_{m,n=1}^{\infty} D(m, n) \cos\left(\frac{m\pi x}{a}\right) \cos\left(\frac{n\pi y}{b}\right) \exp(-\gamma_{mn} z) \tag{2.7b}$$

Form Maxwell's equations

$$\text{Curl } \underline{E} = \nabla \times \underline{E} = -j\omega\mu\underline{H} = -B, t \tag{2.8a}$$

$$\text{Curl } \underline{H} = \nabla \times \underline{H} = -j\omega\epsilon\underline{E} = J + D, t \tag{2.8b}$$

Solution of above equations is based on separation of variables solving LHS of both sides first

$$\nabla \times E = \begin{vmatrix} i & j & k \\ \frac{\partial}{\partial x} & \frac{\partial}{\partial y} & \frac{\partial}{\partial z} \\ E_x & E_y & E_z \end{vmatrix} = i\left(\frac{\partial E_z}{\partial y} - \frac{\partial E_y}{\partial z}\right) - j\left(\frac{\partial E_z}{\partial x} - \frac{\partial E_x}{\partial z}\right) + k\left(\frac{\partial E_y}{\partial x} - \frac{\partial E_x}{\partial y}\right) \tag{2.9a}$$

$$\nabla \times H = \begin{vmatrix} i & j & k \\ \frac{\partial}{\partial x} & \frac{\partial}{\partial y} & \frac{\partial}{\partial z} \\ H_x & H_y & H_z \end{vmatrix} = i\left(\frac{\partial H_z}{\partial y} - \frac{\partial H_y}{\partial z}\right) - j\left(\frac{\partial H_z}{\partial x} - \frac{\partial H_x}{\partial z}\right) + k\left(\frac{\partial H_y}{\partial x} - \frac{\partial H_x}{\partial y}\right) \tag{2.9b}$$

Comparing with RHS in both equations and getting value of H_x, H_y, H_z from (2.9a) and E_x, E_y, E_z from (2.9b) we get

$$H_x = \frac{1}{-j\omega\mu}\left(\frac{\partial E_z}{\partial y} - \frac{\partial E_y}{\partial z}\right); \quad E_x = \frac{1}{j\omega\epsilon}\left(\frac{\partial H_z}{\partial y} - \frac{\partial H_y}{\partial z}\right); \tag{2.10a}$$

$$H_y = \frac{1}{j\omega\mu}\left(\frac{\partial E_z}{\partial x} - \frac{\partial E_x}{\partial z}\right); \quad E_y = \frac{1}{-j\omega\epsilon}\left(\frac{\partial H_z}{\partial x} - \frac{\partial H_x}{\partial z}\right); \tag{2.10b}$$

$$H_z = \frac{1}{-j\omega\mu}\left(\frac{\partial E_y}{\partial x} - \frac{\partial E_x}{\partial y}\right); \quad E_z = \frac{1}{j\omega\epsilon}\left(\frac{\partial H_y}{\partial x} - \frac{\partial H_x}{\partial y}\right); \tag{2.10c}$$

$$E_{z,y} + \gamma E_y = -j\omega\mu H_x$$

$$\gamma E_x + E_{z,x} = j\omega\mu H_y$$

$$H_{z,y} = \frac{\partial H_z}{\mathrm{d}y}$$

$$H_{z,x} = \frac{\partial H_z}{\mathrm{d}x}$$

Similarly,

$$H_{z,y} + \gamma H_y = j = j\omega\epsilon E_x$$

$$\gamma E_x + H_{z,x} = -j\omega\epsilon E_y$$

These above equations can be placed in matrix form

$$\begin{bmatrix} j\omega\epsilon & -\gamma \\ \gamma & -j\omega\mu \end{bmatrix} \begin{bmatrix} E_x \\ H_y \end{bmatrix} = \begin{bmatrix} H_{z,y} \\ -E_{z,x} \end{bmatrix}$$

and

$$\begin{bmatrix} j\omega\epsilon & x \\ \gamma & -j\omega\mu \end{bmatrix} \begin{bmatrix} E_y \\ H_x \end{bmatrix} = \begin{bmatrix} -H_{z,x} \\ E_{z,x} \end{bmatrix}$$

On manipulating them

$$\begin{bmatrix} E_y \\ H_x \end{bmatrix} = \begin{bmatrix} j\omega\mu & -\gamma \\ -\gamma & j\omega\epsilon \end{bmatrix} \begin{bmatrix} -H_{z,x} \\ E_{z,y} \end{bmatrix}$$

Hence, on simplification

$$E_y = \frac{j\omega\mu}{h_{m,n}^2} H_{z,x} - \frac{\gamma}{h_{m,n}^2} E_{z,y}$$

$$\begin{aligned} E_x &= \sum_{m,n} j\omega\mu \frac{\left[D(m,n)\left(\frac{n\pi}{b}\right)\cos\left(\frac{m\pi x}{a}\right)\sin\left(\frac{n\pi y}{b}\right)e^{(-\gamma_{mn}z)}\right]}{h_{m,n}^2} \\ &\quad + \sum \gamma \frac{\left[C(m,n)\left(\frac{m\pi}{a}\right)\cos\left(\frac{m\pi x}{a}\right)\sin\left(\frac{n\pi y}{b}\right)e^{(-\gamma_{mn}z)}\right]}{h_{m,n}^2}; \\ &= \sum_{m,n} j\omega\mu \frac{\left[D(m,n)\left(\frac{n\pi}{b}\right) + \gamma C(m,n)\left(\frac{m\pi}{a}\right)\right.}{h_{m,n}^2} \cos\left(\frac{m\pi x}{a}\right)\sin\left(\frac{n\pi y}{b}\right)e^{(-\gamma_{mn}z)}\Big) \end{aligned} \tag{2.11}$$

Similarly, we can compute

$$\gamma_{m,n}^2 + k^2 = h_{m,n}^2; \quad k^2 = \mu\epsilon\omega^2$$

$$h_{m,n}^2 = \left(\frac{m\pi}{a}\right)^2 + \left(\frac{n\pi}{b}\right)^2$$

$$\gamma_{mn} \rightarrow \text{propagation constant}$$

$$\begin{aligned} E_{ix}(m,n) &= \frac{2}{ab}\int_0^a \int_0^b E_{ix}(x,y)\cos\left(\frac{m\pi x}{a}\right)\sin\left(\frac{n\pi y}{b}\right)\mathrm{d}x\mathrm{d}y \\ &= \frac{j\omega\mu\left(\frac{n\pi}{b}\right)D(m,n) + \gamma_{m,n}C(m,n)\left(\frac{m\pi}{a}\right)}{h_{m,n}^2}; \end{aligned} \tag{2.12a}$$

$$\begin{aligned} E_{iy}(m,n) &= \frac{2}{ab}\int_0^a \int_0^b E_{iy}(x,y)\sin\left(\frac{m\pi x}{a}\right)\cos\left(\frac{n\pi y}{b}\right)\mathrm{d}x\mathrm{d}y \\ &= -\left(\frac{j\omega\mu}{h_{m,n}^2}D(m,n)\left(\frac{m\pi}{a}\right) + \frac{\gamma_{m,n}C(m,n)\,\frac{n\pi}{b}}{h_{m,n}^2}\right); \end{aligned} \tag{2.12b}$$

$$\begin{bmatrix} E_{ix}(m,n) \\ E_{iy}(m,n) \end{bmatrix} = \begin{bmatrix} \frac{m\pi}{a}\frac{\gamma_{m,n}}{h_{m,n}^2} & \frac{n\pi}{b}\frac{j\omega\mu}{h_{m,n}^2} \\ -\frac{\gamma_{m,n}}{h_{m,n}^2}\frac{n\pi}{b} & -\frac{j\omega\mu}{h_{m,n}^2}\frac{m\pi}{a} \end{bmatrix} \begin{bmatrix} C(m,n) \\ D(m,n) \end{bmatrix}$$

Hence, $C(m,n), D(m,n)$ amplitude coefficients can be computed, when the boundary conditions are given as:

$$\left\{ \begin{array}{l} x = 0, a \\ y = 0, b \\ z = 0, d \end{array} \right\}$$

Incident waves at input of waveguide are $E_{ix}(x,y)$, $E_{iy}(x,y)$

$$E_{ix}(x,y) = \sum_{m,n} \frac{j\omega\mu D(m,n)\left(\frac{n\pi}{b}\right) + \gamma_{m,n} C(m,n)\left(\frac{m\pi}{a}\right)}{h_{m,n}^2} \left[\cos\left(\frac{m\pi x}{a}\right)\sin\left(\frac{n\pi y}{b}\right)\right]; \tag{2.13a}$$

$$E_{iy}(x,y) = \sum_{m,n} \frac{j\omega\mu D(m,n)\left(\frac{m\pi}{a}\right) + \gamma_{m,n} C(m,n)\left(\frac{n\pi}{b}\right)}{h_{m,n}^2} \left[\sin\left(\frac{m\pi x}{a}\right)\cos\left(\frac{n\pi y}{b}\right)\right]. \tag{2.13b}$$

2.5 Two-Dimensional Resonator

Solution is obtained by the application of Helmholtz equation.

$$\frac{\partial^2\psi(x,y,t)}{\partial x^2} + \frac{\partial^2\psi(x,y,t)}{\partial y^2} - \frac{1}{c^2}\frac{\partial^2\psi(x,y,t)}{\partial t^2} = 0 \tag{2.14}$$

Applying boundary conditions in rectangular plane,

$$\psi(0,y,t) = \psi(a,y,t) = 0$$

$$\psi(x,0,t) = \psi(x,b,t) = 0$$

Let input excitation be some tension T

$$\sigma \mathrm{d}x\mathrm{d}y \frac{\partial^2\psi}{\partial t^2} = \frac{\partial}{\partial x}\left(T \cdot \mathrm{d}y \frac{\partial\psi}{\partial x}\right)\mathrm{d}x + \frac{\partial}{\partial y}\left(T \cdot \mathrm{d}x \frac{\partial\psi}{\partial y}\right)\mathrm{d}y \tag{2.15}$$

$$\frac{Y''}{Y} = -k_y^2; \qquad \frac{X''}{X} = -k_x^2;$$

$$\frac{\partial^2 \psi}{\partial t^2} - c^2 \nabla^2 \psi = 0 \tag{2.16}$$

Using separation of variables:

$$\psi(x, y, t) = X(x)Y(y)T(t) \tag{2.17}$$

$$-\omega^2 = \frac{T''(t)}{T(t)} = c^2 \left(\frac{X''(x)}{X(x)} + \frac{Y''(y)}{Y(y)} \right)$$

let

$$X(x) = \sin(k_x x)$$

$$Y(y) = \sin(k_y y)$$

$$k_x^2 + k_y^2 = \frac{\omega^2}{c^2}$$

where k_x and k_y can be written as:

$$k_x = \frac{m\pi}{a}; \quad k_y = \frac{n\pi}{b} \tag{2.18}$$

Frequency can be written as: $\omega(mn) = c\pi \sqrt{\left(\frac{m}{a}\right)^2 + \left(\frac{n}{b}\right)^2}$.

2.6 Basic Mathematical Representation of Resonant Modes

$$\nabla^2 A_x + k^2 A_x = 0; \tag{2.19}$$

$k_r \gg 1$ far field pattern
$k_r \ll 1$ near field pattern

where A_z is the magnetic vector potential and k is the wave vector or wave number along z-axis.

$$A_z = (C_1 \cos(k_x x) + C_1 \sin(k_x x))(C_3 \cos(k_y y) + C_4 \sin(k_y y))(C_5 \cos(k_z z) + C_6 \sin(k_z z));$$

$$A_z = \frac{\mu}{4\pi}\int J(z')\frac{e^{jkR}}{R}d^3z'; \qquad (2.20)$$

$$k_c = \frac{2\pi}{\lambda},\ k_0 = \sqrt{k_x^2 + k_y^2 + k_z^2} = \omega^2\epsilon\mu, \text{ where } k \text{ is the wave number.}$$

The wave number can be defined as rate of change of phase w.r.t. distance in the direction of propagation. Resonant frequency $\omega = \omega_{mnp}$ in RDRA and its mathematical expression is given below:

$$(f_r)m,n,p = \frac{c}{\sqrt[2\pi]{\varepsilon_r}}\sqrt{\left(\frac{m\pi}{a}\right)^2+\left(\frac{n\pi}{b}\right)^2+\left(\frac{p\pi}{d}\right)^2}; \qquad (2.21)$$

where m, n, p are the half-wave field variations along x, y, z directions.

$H = \nabla \times A$

$E = -\nabla ø - \frac{\mathrm{d}A}{\mathrm{d}t}$; scalar and magnetic vector potential from Lorentz Gauge conditions.

$S = (E \times H^*)$; S is Poynting vector (energy flow or flux).

$Z = \frac{P_{\mathrm{rad}}}{|I|^2}$ = input Impedance.

$E_x, E_y, E_z, H_x, H_y, H_z$ are electric and magnetic fields

$$\mathcal{L}\oint\left\{\cos\left(\frac{n\pi x}{a}\right), \sin\left(\frac{n\pi x}{a}\right)\right\} \otimes \mathcal{L}\oint\left\{\cos\left(\frac{m\pi y}{b}\right), \sin\left(\frac{m\pi y}{b}\right)\right\}; \qquad (2.22)$$

where $\mathcal{L}$ denotes linear components. It turns out that depending on the nature of wall surfaces (PEC or PMC), four possible linear combinations can appear $(\cos\otimes\sin, \sin\otimes\cos, \sin\otimes\sin,\ \text{and}\ \cos\otimes\cos)$.

In rectangular DRA, we've got to applying in additional boundary conditions on top and bottom surfaces to be the linear combinations as compared to waveguide.

$$C_1\exp\{(-\gamma(m,n,\omega)z\} + C_2\exp\{+\gamma(m,n,\omega)z\}$$

and these cases are $\gamma(m,n,\omega) = \frac{\pi p}{d}$, when $p = 1,2,3\ldots$ and have two possible linear combinations of $\sin\left(\frac{\pi pz}{d}\right)$ and $\cos\left(\frac{\pi pz}{d}\right)$.

Thus, the possible frequencies ω obtained by solving $\gamma(m,n,\omega) = \frac{\pi p}{d}$; then comes out to be:

$$\omega(m,n,p) = \pi\left[\frac{m^2}{a^2}+\frac{n^2}{b^2}+\frac{p^2}{d^2}\right]^{1/2}. \qquad (2.23)$$

An equivalent but computationally simpler way to pass on from waveguide physics to resonator physics is to just replace γ by $-\frac{\partial}{\partial z}$ in all the waveguide formulae that express the tangential field components in terms of the longitudinal components. This is done after solving the full 3-D Helmholtz equations using separation of variable in x, y, z.

$$\left(\nabla^2 + \frac{\omega^2}{c^2}\right)\begin{pmatrix} E_z \\ H_z \end{pmatrix} = 0 \tag{2.24}$$

The discrete modes ω_{mnp} enable us to visualize the resonator as collection of L, C oscillators with different L, C values. The outcome of all this analysis enables us to write down the $\underline{E}$ and $\underline{H}$ fields inside the resonator, as superposition of four, three vector-valued basis functions.

$$\begin{aligned} \underline{E}(x,y,z,t) = {} & \sum_{mnp=1}^{\infty} \mathrm{Re}\left\{C_{mnp} e^{j\omega(mnp)t} \underline{\psi}^{E}_{mnp}(x,y,z)\right\} \\ & + \sum_{mnp=1}^{\infty} \mathrm{Re}\left\{D_{mnp} e^{j\omega(mnp)t} \underline{\bar{\phi}}^{E}_{mnp}(x,y,z)\right\}; \end{aligned} \tag{2.25}$$

and

$$\begin{aligned} \underline{H}(x,y,z,t) = {} & \sum_{mnp=1}^{\infty} \mathrm{Re}\left\{C(mnp) e^{j\omega(mnp)t} \underline{\psi}^{H}_{mnp}(x,y,z)\right\} \\ & + \sum_{mnp=1}^{\infty} \mathrm{Re}\left\{D(mnp) e^{j\omega(mnp)t} \underline{\bar{\phi}}^{H}_{mnp}(x,y,z)\right\}; \end{aligned} \tag{2.26}$$

We note that there are only two sets $\{C_{mnp}\}$ and $\{D_{mnp}\}$ of linear combination of coefficients from the E_z and H_z *expansions*. The vector-valued complex functions are $\underline{\psi}^{E}_{mnp}$, $\underline{\bar{\phi}}^{E}_{mnp}$ $\underline{\psi}^{H}_{mnp}$ $\underline{\bar{\phi}}^{H}_{mnp} \in R^3$ (where R is autocorrelation) and contains components $\{\cos,\sin\} \otimes \{\cos,\sin\} \otimes \{\cos,\sin\}$, functions and hence for $(m'n'p') \neq (mnp)$, each function of the set:

$$\left\{\underline{\psi}^{E}_{mnp}, \underline{\bar{\phi}}^{E}_{mnp}, \underline{\psi}^{H}_{mnp}, \underline{\bar{\phi}}^{H}_{mnp}\right\};$$

is orthogonal to each functions of the set:

$$\left\{\underline{\psi}^{E}_{m'n'p}, \underline{\bar{\phi}}^{E}_{m'n'p}, \underline{\psi}^{H}_{mnp}, \underline{\bar{\phi}}^{H}_{m'n'p}\right\};$$

w.r.t. the measure of dx dy dz over [0, a] × [0, b] × [0, d].

The exact form of the function $\underline{\bar{\phi}}^{E}$, $\underline{\bar{\phi}}^{H}$, $\underline{\psi}^{E}$, $\underline{\psi}^{H}$ depends on the nature of the boundaries. The next problem addressed can be on excitations of RDRA. To calculate the amplitudes' coefficients $\{C_{mnp}\}$ and $\{D_{mnp}\}$, we assume that at $z = 0$, excitations $E_x^{(e)}(x, y, t)$ or $E_y^{(e)}(x, y, t)$ are applied for some time say $t \in [0, T]$ and then removed. Then, the Fourier components in this excitation corresponding to the frequencies $\omega\{(mnp)\}$ are excited and their solutions are the oscillations, while the waveguide for $t > T$. The other Fourier components decay within the resonator.

$\{C_{mnp}, D_{mnp}\}$ are the components of the form:

$$E_x^{(e)}(x, y, t) = \sum_{mnp} \mathrm{Re}\Big(C(mnp)e^{j\omega(mnp)t}\psi^{E}_{mnp\,x}(x, y, 0)\Big) + \mathrm{Re}\Big(D(mnp)e^{j\omega(mnp)t}\underline{\bar{\phi}}^{E}_{mnp\,x}(x, y, 0)\Big) \tag{2.27}$$

and

$$E_y^{(e)}(x, y, t) = \sum_{mnp} \mathrm{Re}\Big(C(mnp)e^{j\omega(mnp)t}\psi^{E}_{mnp\,y}(x, y, 0)\Big) + \mathrm{Re}\Big(D(mnp)e^{j\omega(mnp)t}\underline{\bar{\phi}}^{E}_{mnp\,y}(x, y, 0)\Big); \tag{2.28}$$

By using, orthogonality of $\{\psi^{E}_{mnp\,x}(x, y, 0), \underline{\bar{\phi}}^{E}_{mnp\,x}(x, y, 0)\}$. For different (m, n), we write p to be fixed and likewise of $\{\psi^{E}_{mnp\,y}(x, y, 0), \underline{\bar{\phi}}^{E}_{mnp\,y}(x, y, 0)\}$.

In addition, we need to use KAM type of time averaging to yield field components:

$$C(mnp)\psi^{E}_{mnp\,x}(x, y, 0) + D(mnp)\underline{\bar{\phi}}^{E}_{mnp\,x}(x, y, 0) = \lim_{T\to\infty} \frac{1}{2T}\int_{-T}^{T} E_x^{(e)}(x, y, t)e^{-j\omega(mnp)t}\mathrm{d}t. \tag{2.29}$$

and likewise

$$C(mnp)\psi^{E}_{mnp\,y}(x, y, 0) + D(mnp)\underline{\bar{\phi}}^{E}_{mnp\,y}(x, y, 0) = \lim_{T\to\infty} \frac{1}{2T}\int_{-T}^{T} E_y^{(e)}(x, y, t)e^{j\omega(mnp)t}\mathrm{d}t. \tag{2.30}$$

2.7 Voltage Source Model

This method of excitation can be compared with connecting a voltage or current source to an LC circuit for sometimes and then switching it off. After a sufficiently long time, all frequencies in the LC circuit decay away except the frequency $\frac{1}{\sqrt{LC}}$. We can more generally compare a resonator with the material medium having non-zero conductivity. Thus, the medium is characterized by the triplet $(\epsilon, \beta, \sigma)$ which corresponds to an array of (C, L, R) = RLC circuits.

Such a resonator is analyzed in the same way replacing ϵ by $\epsilon' = \epsilon - \frac{j\sigma}{\omega}$, i.e., complex permittivity depending on frequency. The resonant frequencies $\omega(mnp)$ now have a non-zero imaginary part corresponding to decay of the field with time. Their frequencies and fields may also be determined by applying separation of variables with boundary conditions to the Helmholtz equations.

$$[\nabla^2 - j\omega\mu(\sigma + j\omega\epsilon)]\begin{bmatrix} E_z \\ H_z \end{bmatrix} = 0; \tag{2.31}$$

To have sustained oscillations in such a resonator, we must never switch off the excitation. We may for example apply a surface current source at $z = \delta_0$, where $0 < \delta_0 \ll d$. Letting $J_{sx}(x, y, \omega)$ and $J_{sy}(x, y, \omega)$ be this surface current excitations in the Fourier domain, the current density corresponds to this is given as:

$$\underline{J}_e(x, y, z, \omega) = (J_{sx}(x, y, \omega)\hat{X} + J_{sy}(x, y, \omega)\hat{Y}\,\delta(z - \delta_0); \tag{2.32}$$

This current is computed by substituting into the Maxwell curl equations

$$\text{Curl}\,\underline{E} = -j\omega\mu\,\underline{H},$$

$$\text{Curl}\,\underline{H} = \underline{J}_e + (\sigma + j\omega\epsilon)\underline{E},\ \text{div}\,\underline{H} = 0$$

The method of solution is to express it as the sum of a general solution to the homogeneous equations, i.e., with $\underline{J}_e = 0$ and a particular solutions for $\underline{J}_e \neq 0$. The general solutions to the homogeneous problem are the same as earlier explained, i.e., containing only the frequencies $\{\omega(mnp)\}$. Particular solution to the $\underline{J}_e \neq 0\,(inhomogenous)$ problem is obtained by taking the curl of the second equation and substituting the fields into third equation to obtain

$$\nabla^2\underline{H} = -\underline{\nabla} \times \underline{J}_e + j\omega\mu(\sigma + j\omega\epsilon)\underline{H}; \tag{2.33}$$

We express a particular solution to this equation by setting

$$\sum_{m,n=1}^{\infty} (\mathcal{L}_1(m,n,\omega)\exp(-\gamma(mn\omega)z)\underline{u}_{mn}(x,y,\omega) \\ + \beta_1(m,n,\omega)\exp(\gamma(mn\omega)z)\underline{v}_{mn}(x,y,\omega) \quad \text{for } d \geq z > \delta; (2.14) \tag{2.34a}$$

$$\underline{H}_p(x,y,z,\omega) = \sum_{m,n=1}^{\infty} (\mathcal{L}_2(m,n,\omega)\exp - \gamma(mn\omega)z)\underline{u}_{mn}(x,y,\omega) \\ + \beta_2(m,n,\omega)\exp(\gamma(mn\omega)z)\underline{v}_{mn}(x,y,\omega) \quad \text{for } 0 \leq z < \delta; (2.15) \tag{2.34b}$$

Here, ω is a continuous variable, unlike $\{\omega(mnp)\}$, $\underline{u}_{mn}(x,y,\omega)$ and $\underline{v}_{mn}(x,y,\omega)$ are multiples (ω-dependent) of

$$\mathcal{L}\left\{\cos\left(\frac{m\pi x}{a}\right), \sin\left(\frac{n\pi x}{a}\right)\right\} \otimes \mathcal{L}\left\{\cos\left(\frac{m\pi y}{p}\right), \sin\left(\frac{m\pi y}{p}\right)\right\}$$

To meet the boundary conditions on the sidewalls, if $z = 0$, d; if the walls are PEC, $H_{pz} = 0$; when $z = 0$, d. That gives use

$$H_{pz}(x,y,z,\omega) = \sum_{m,n} \mathcal{L}(m,n,\omega)\sin h\{\gamma(m,n,\omega)(z-d)\}\underline{u}_{mnz}(x,y,\omega), \quad \delta < z \leq d; \tag{2.35}$$

and

$$H_{pz}(x,y,z,\omega) = \sum_{m,n} \beta(m,n,\omega)\sin h\{\gamma(m,n,\omega)z)\}\underline{u}_{mnz}(x,y,\omega), \quad 0 \leq z < \delta; \tag{2.36}$$

The fields $H_{p\perp}(x,y,z,\omega)$ are easily determined from these equations in the region $z > \delta$ and $z < \delta$ by differentiating them w.r.t. x, y, z; wherever γ comes in the multiple w.r.t. $\exp(-\gamma z)$, we replace it by $-\frac{\partial}{\partial z}$ etc.

In this way, we get

$$H_{px}(x,y,z,\omega) = \sum_{m,n=1}^{\infty} \mathcal{L}_1(m,n,\omega)\psi_{mnx}(x,y,z,\omega), \quad \text{for } z > \delta; \tag{2.37a}$$

and

$$H_{py}(x,y,z,\omega) = \sum_{m,n=1}^{\infty} \mathcal{L}_2(m,n,\omega)\psi_{mny}(x,y,z,\omega), \quad \text{for } z < \delta; \tag{2.37b}$$

where, $\psi_{mnx}(x, y, z, \omega)$ and $\psi_{mny}(x, y, z, \omega)$ are obtained by differentiating

$$\underline{u}_{mnz}(x, y, \omega) \sin h\{\gamma(m, n, \omega)(z - d)\} \quad \text{w.r.t. } x, y, z.$$

Likewise for $z < \delta$, we have expression of the form

$$H_{px}(x, y, z, \omega) = \sum_{m,n=1}^{\infty} \beta(m, n, \omega) \underline{\bar{\phi}}^{E}_{mnp\,x}(x, y, z, \omega); \tag{2.38a}$$

and

$$H_{py}(x, y, z, \omega) = \sum_{m,n=1}^{\infty} \beta(m, n, \omega) \underline{\bar{\phi}}^{E}_{mnp\,y}(x, y, z, \omega); \tag{2.38b}$$

The coefficients $\mathcal{L}(m, n, \omega)$ and $\beta(m, n, \omega)$ are obtained from the boundary conditions

$$\hat{z} \times \left(H|_{z=\delta+} - H|_{z=\delta-} \right) = J_s|_{z=\delta+}.$$

Hence, current density

$$J = J_{sx}(x, y, \omega)\hat{X} + J_{sy}(x, y, \omega)\hat{Y}. \tag{2.39}$$

2.8 Resonant Modes Generation

The Fig. 2.2 presents how the generated modes look like. This will be able to tell us the number of resonant modes in particular direction. The transverse components of EM waves are expressed as E_x, E_y, H_x, H_y. If propagation of wave is along z-direction, E_z, H_z fields are the longitudinal components. These fields are modal solutions, solved based on Helmholtz equations using standard boundary conditions. The RDRA is basically a boundary value problem. The linear combinations of sine and cosine terms give rise to TE and TM modes. The generation of various kinds of modes in an antenna and propagation is very critical issue; it need through study. Now, rewriting Helmholtz equation for source-free medium (Fig. 2.3)

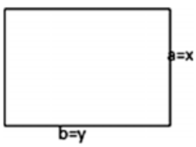

Fig. 2.2 Rectangular resonator

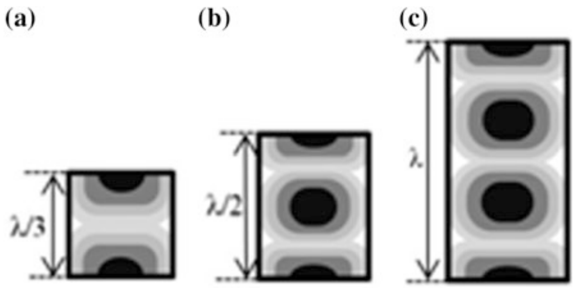

Fig. 2.3 Resonant modes generated in RDRA by HFSS. **a** $TE^x_{\delta 12}$, **b** $TE^x_{\delta 14}$, **c** $TE^x_{\delta 16}$ modes

$$\nabla^2 \Psi + k^2 \Psi = 0,$$

Here, k is the wave number and $k^2 = k_x^2 + k_y^2 + k_z^2$ and, $\Psi = \Psi_x \cdot \Psi_y \cdot \Psi_z$

$$\frac{1}{\Psi_x}\left(\frac{\partial}{\partial x}\right)^2 \Psi = -k_x^2 \tag{2.40a}$$

$$\frac{1}{\Psi_y}\left(\frac{\partial}{\partial y}\right)^2 \Psi = -k_y^2 \tag{2.40b}$$

$$\frac{1}{\Psi_z}\left(\frac{\partial}{\partial z}\right)^2 \Psi = -k_z^2 \tag{2.40c}$$

Solving above function and keeping propagation in +z-direction only, we get

$$\Psi \text{ or } H_z \text{ or } E_z = \left\{(A \sin k_x \cdot x + B \cos k_x \cdot x)\left(C \sin k_y \cdot y + D \cos k_y \cdot y\right)\right\} e^{-jk_z z}$$

From boundary conditions, we get

$$H_z = \sum_{m,n} \left\{ C_{mn}\left(\cos\frac{m\pi x}{a}\right)\left(\cos\frac{n\pi y}{b}\right)\right\} e^{-jk_z z}; \quad C_{mn} \text{ Fourier Coefficients;} \tag{2.41a}$$

$$E_z = \sum_{m,n} \left\{ D_{mn}\left(\sin\frac{m\pi x}{a}\right)\left(\sin\frac{n\pi y}{b}\right)\right\} e^{-jk_z z}; \quad D_{mn} \text{ Fourier Coefficients;} \tag{2.41b}$$

Let $\gamma = -jk_z$ and m, n are integers and a, b are dimensions;

$$\gamma^2 + \omega^2 \mu \epsilon = k_x^2 + k_y^2 = \left(\frac{m\pi}{a}\right)^2 + \left(\frac{n\pi}{b}\right)^2$$

$$k_z^2 = \omega^2 \mu \epsilon - \left(\left(\frac{m\pi}{a}\right)^2 + \left(\frac{n\pi}{b}\right)^2\right)$$

Hence, EM wave will propagate in z-direction if

$$\omega^2\mu\epsilon - \left(\left(\frac{m\pi}{a}\right)^2 + \left(\frac{n\pi}{b}\right)^2\right) > 0$$

This gives cutoff frequency as

$$\omega_c = \frac{1}{\sqrt{\mu\epsilon}}\sqrt{\left(\left(\frac{m\pi}{a}\right)^2 + \left(\frac{n\pi}{b}\right)^2\right)}$$

It means, waveguide will support all waves having ω greater than ω_c to propagate.
Now, rewriting H_z and E_z

$$H_z = \sum_{m,n}\left\{C_{mn}\left(\cos\frac{m\pi x}{a}\right)\left(\cos\frac{n\pi y}{b}\right)\right\}e^{-jk_z z} \quad (2.42)$$

$$E_z = \sum_{m,n}\left\{D_{mn}\left(\sin\frac{m\pi x}{a}\right)\left(\sin\frac{n\pi y}{b}\right)\right\}e^{-jk_z z} \quad (2.43)$$

Here, C_{mn} and D_{mn} are the coefficients of Fourier cosine and sine series.

$$\gamma_{m,n} = \sqrt{h^2_{m,n} - \omega^2\mu\varepsilon}$$

Hence, C_{mn} and D_{mn} gives us relative amplitudes and phase. Hence, we get solution of possible amplitudes and phase of wave propagating through rectangular waveguide called as modes of propagation.

2.9 MATLAB Simulated Results

Results of resonant frequency obtained on various sizes RDRA's using HFSS have been placed in Table 2.1. The MATLAB programs are being developed for modes graphical view. Resonant modes and resonant frequencies are being obtained based on formulations. The programs and simulated results are given below:

MATLAB program no.1

```
clearall;
clc;
closeall;
c=3*10^8;
m=7;
n=10;
p=6;
E=10;
```

```
a=5*10^-3:.1*10^-3:30*10^-3;
b=10*10^-3;
d=15*10^-3;

for i=1:length(a)
f(i)=c/(2*pi)*sqrt(E)*sqrt((m*pi/a(i))^2+(n*pi/b)^2+(pp*pi/(2*d)^2));
end

a1=15*10^-3;
b1=10*10^-3:.1*10^-3:40*10^-3;
d1=20*10^-3;

for k=1:length(b1)
f1(k)=c/(2*pi)*sqrt(E)*sqrt((m*pi/a1)^2+(n*pi/b1(k))^2+(pp*pi/(2*d1)^2));
end

a2=10*10^-3;
b2=5*10^-3;
d2=10*10^-3:.1*10^-3:50*10^-3;

for t=1:length(d2)
f2(t)=c/(2*pi)*sqrt(E)*sqrt((m*pi/a2)^2+(n*pi/b2)^2+(pp*pi/(2*d2(t))^2));
end

subplot(3,1,1);plot(a,f);title('plot a vs f when a is varying');
subplot(3,1,2);plot(b1,f1);title('plot b vs f when b is varying');
subplot(3,1,3);plot(d2,f2);title('plot d vs f when d is varying');
```

Table 2.1 RDRA HFSS f_r

S. No.	Permittivity	Dimension ($a \times b \times h$) mm	Resonant frequency
1	10.0	14.3 × 25.4 × 26.1	3.5
2	10.0	14 × 8 × 8	5.5
3	10.0	15.24 × 3.1 × 7.62	6.21
4	20.0	10.2 × 10.2 × 7.89	4.635
5	20.0	10.16 × 10.2 × 7.11	4.71
6	35.0	18 × 18 × 6	2.532
7	35.0	18 × 18 × 9	2.45
8	100.0	10 × 10 × 1	7.97

The graph shown in Fig. 2.4 represents inverse relationship between height and resonant frequency as λ-wavelength is inversely proportional to resonant frequency fr. MATLAB simulation shown in Fig. 2.5 represents number of modes generated in x, y, z directions. The mathematical expression on the topic is expressed in Eqs. (2.1)–(2.31).

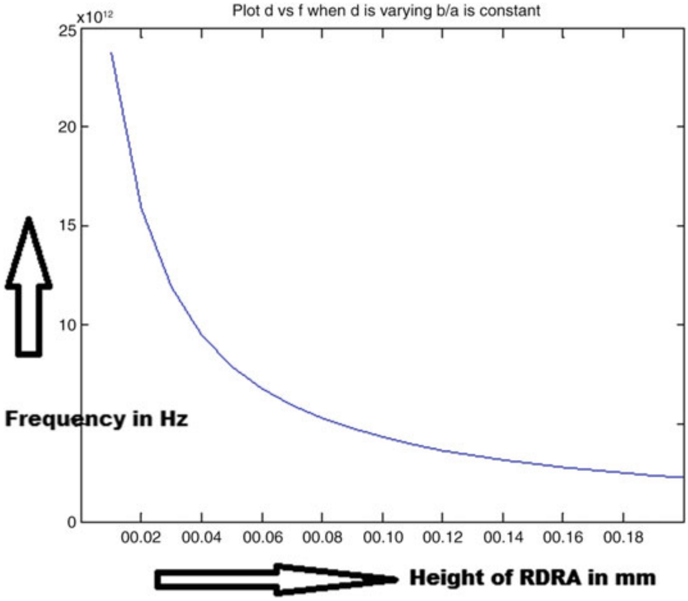

Fig. 2.4 Simulated resonant frequency plot for excited modes

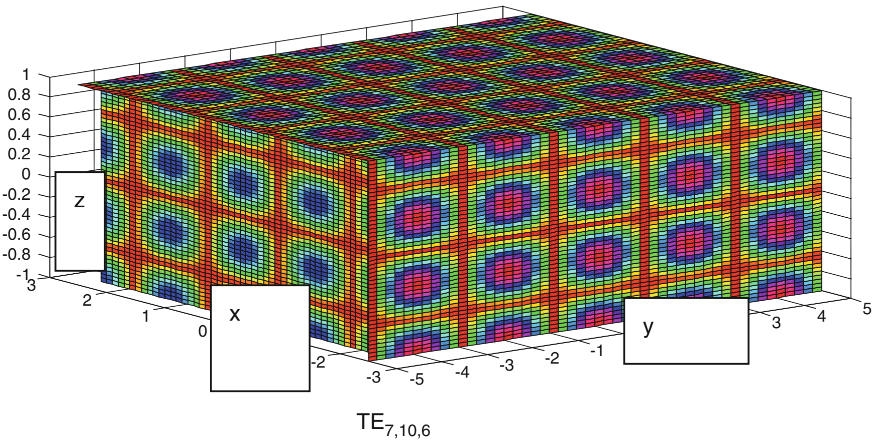

Fig. 2.5 Resonant modes 3D in RDRA in *xyz* plane

MATLAB Program2

```
m=5;
n=4;
p=3;
a=10;
b=5;
c=2;
x=linspace(-5,5,51);
y=linspace(-2.5,2.5,51);
z=linspace(-1,1,51);
[xi,yi,zi] = meshgrid(x,y,z);
Ez= (cos(m*pi*xi/a).*cos(n*pi*yi/b)).*sin(p*pi*zi/c);
Ez= Ez.^2;
Ez= sqrt(Ez);
xslice = -4.5; yslice = -2.5; zslice =1;
slice(xi,yi,zi,Ez,xslice,yslice,zslice)
colormap hsv
```

Reference

1. Okaya A, Barash LF (1962) The dielectric microwave resonator. Proc IRE 50:2081–2092